

Electromagnetic Paper Drying

J. Cesar Monzon, *Member, IEEE*

Abstract—A solution to the nonlinear problem of drying of a sheet material is presented, which combines basic thermodynamic properties with the field equations. Some results are given in a numerical simulation.

I. INTRODUCTION

WORKS ON microwave heating are abundant in the literature basically because of the important problem of the localization of power deposition in living tissues. When irradiating living tissues we are dealing with low powers, and the usual theoretical approach is that of linearized equations where the target is characterized by constant electrical parameters, e.g. [1], [2]. Note that the common objective is to heat the target or part of the target (tumor for example). However, with continuous irradiation the energy loss increases without limits which indicates that even for low powers the heating problem is nonlinear when seen in an appropriate time scale. It should be mentioned that a formal solution must account for surface cooling of the target [3]; and if dealing with a live target, the internal cooling effect of the blood circulation must be accounted for.

By contrast with the above, the literature on analytical works on microwave drying is very limited. The drying problem is eminently nonlinear. One of the most important problems of industrial microwave systems relates to thin web or sheet materials [4].

Here we present some results of our study [10] in the use of electromagnetic fields to dry thin structures such as wet paper, in a continuous manner. This work has concentrated on an elementary technique for estimating the temperature and moisture profiles based on a rigorous field solution. Thus, we are dealing with the real (highly nonlinear) simulation, where the electrical characteristics of the load depend on the fields.

Aside from ignoring material anisotropies, a problem which we have not investigated is that of inhomogeneities (both of illumination and of geometry), which is quite important since it can lead to hot spots and thermal gradients which can result in damage to the material being dried. This work is based on the assumptions of homogeneous isotropic materials and homogeneous illumination. We also assume that the losses in the material be mainly dependent on the free water content and not on ionic conduction (which occurs at low frequencies and depends strongly upon the chemical composition of the host material). Qualitatively it is known [13], that these two effects usually occur in different frequency ranges. Thus, in a sense, our analytical assumption is a constraint in the range of usable frequencies and possibly also in moisture levels.

Manuscript received July 12, 1993; revised April 25, 1994.

The author is with Damaskos, Inc., Concordville, PA 19331 USA.
IEEE Log Number 9407281.

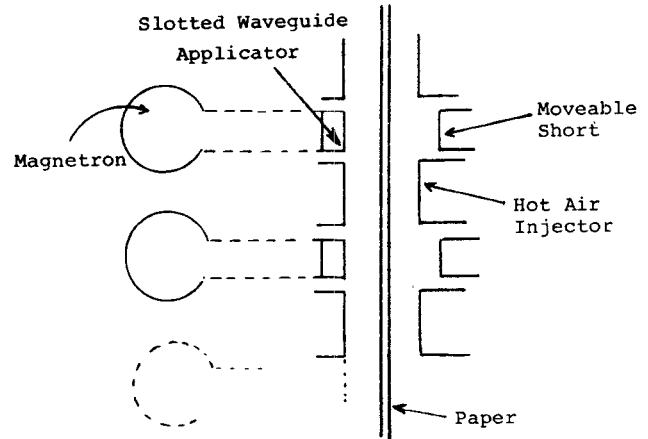


Fig. 1. Proposed arrangement.

To achieve homogeneous illumination it is suggested that an arrangement similar to that of laboratory ovens [5] be employed. The proposed arrangement is shown in Fig. 1, and employs a series of magnetrons, each with tuning elements to allow matching to a wide range of loads. To increase efficiency, the hot air of the magnetrons can be blown onto the material,¹ helping maintain the temperature of the material at a sufficiently high level, and at the same time, helping get rid of the air moisture (which is very significant) in order to avoid condensation. As pointed out by a reviewer, it is also possible to dehumidify the hot moist air discharged by the dryer and recycle its heat [12].

The last point may be quite important in view of the fact that current fabrication processes require the paper to move at a relatively high speed (~ 4.5 m/sec.). This requires very large electric fields with the consequent threat of air breakdown, which is worsened by moisture in the air.

Here we deal with the simplified two dimensional model (of a single element) shown in Fig. 2, where the region of continuous heating is bounded by perfectly conducting half planes which are located at $z = 0$ and $z = h$. T_o and T_i denote the output and input temperatures of the sheet of paper which moves at speed v . The impressed field is that of a plane wave of amplitude E_o , whose electric vector points in the \hat{z} direction. Hot air is assumed to flow between the plates in order to get rid of the moisture. The case of bilateral illumination would not affect the analysis. However, for simplicity only one-sided illumination is employed. It should also be mentioned that the effect of the slots is ignored in this rather crude model. The time convention $\exp\{j\omega t\}$ is assumed and suppressed throughout.

¹The recovery of the heat given off by the magnetron has been claimed in a patent [11].

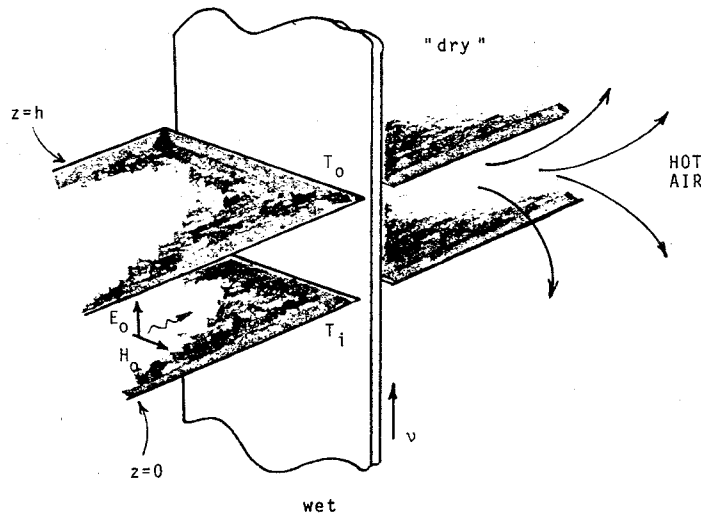


Fig. 2. Simplified two-dimensional model of a single element.

II. ANALYSIS

The electromagnetic properties of the sheet of wet paper are characterized by permeability μ_o and relative permittivity $\epsilon = \epsilon' - j\epsilon''$, which is a function of the temperature (and therefore a function of z). In view of the fact that ϵ for paper is much less than ϵ for water, we shall assume (upon neglect of ionic conduction as pointed out in the introduction) that the sheet can be represented by an inhomogeneous slab of water. Thus it seems convenient to model the "wet" paper by a thin resistive sheet.

We should mention that in reality the bulk ϵ' and ϵ'' do depend on the moisture content. The above slab of water simplification neglects such a dependence. This however is not a crucial point for if an improved functional dependence of ϵ was available, we could use it in the same way we use this one, as will become clear later on. Actually, a physical model of the moisture/density dependence of the dielectric properties of even the simplest natural products is not possible yet. This is the same situation of a decade ago [13], [14]. The dependence is still determined empirically even for single grains [15], [16].

Let d (meters) denote the thickness of the paper which will be assumed to be the same for both wet and dry conditions, and let p denote the initial fractional volume of water, i.e., volume of water/volume of the paper (all per unit area). We now introduce $\rho(z)$, the amount of water per unit area, which will be given in (gr/m^2) . Thus, $\rho(0)$ denotes the amount of water in the wet paper, and is given by

$$\rho(0) = p \cdot d \cdot 10^6 gr/m^2. \quad (1)$$

Similarly, $\rho(h)$ is the amount of water in the "dry" condition. It is known [17] that a thin dielectric sheet can be completely characterized by a (sheet) admittance equal to: $j\omega(\epsilon - 1) \times$ thickness. In view of the above, the equivalent normalized R-sheet value of the paper is:

$$\frac{R(z)}{\eta} = \frac{1}{j\eta k d (\epsilon' - 1 - j\epsilon'')} \cdot \frac{\rho(0)}{\rho(z)} \quad (2)$$

which takes into account the effect of evaporation on the effective thickness of the sheet, and where k denotes the wave

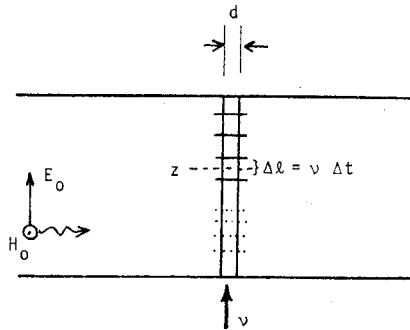


Fig. 3. Discretization employed in the analysis.

number of the impressed electromagnetic field. It should be stressed that ϵ' and ϵ'' depend on the temperature T ($^{\circ}$ C), which is a function of the position (z). η is the free space impedance (376.7Ω) and $R(z)$ is expressed in Ω .

We now refer to Fig. 3, where the paper has been split into numerous strips, each of width Δl . In a time interval $\Delta t = \Delta l/v$, where v is the speed of the paper in (m/sec), each strip will move to the position previously occupied by the adjacent (upper) strip. In a time Δt , a given strip dissipates an amount of microwave energy $\Delta\epsilon(z) = \Delta t \cdot \Delta l \cdot \text{Re}\{E^* \cdot J\}$ (Joules), where J is the current in the R-sheet: $E = J \cdot R$. In view of (2) we get:

$$\Delta\epsilon(z) = \Delta t \cdot \Delta l \cdot \frac{\rho k d}{\eta} \epsilon''(T(z)) \frac{\rho(z)}{\rho(0)} |E(z)|^2 \quad (3)$$

which has been calculated per/meter wide sheet.

Now we proceed to exploit (3) by introducing some thermodynamic properties of the sheet, which will be assumed to be accurately represented by the water properties. First we note that the temperature T will increase from an initial value $T(0) = T_i$ to a maximum² $T_c = 100^{\circ}\text{C}$ at h_c (meters), and will remain at that value for all $z \in (h_c, h)$. This, provided T_c can be reached, otherwise the exit temperature will be T_o .

²The practical maximum is actually material dependent and not much larger than the 100°C (pure water at sea level) adopted here for computational purposes.

Similarly, for $z \in (0, h_c)$, no evaporation can take place which implies $\rho(z) = \rho(0)$. For $z \geq h_c$, evaporation will occur and ρ will decrease.

Based on the above, we can postulate the following behavior:

$$1) z < h_c, T < T_c.$$

The energy $E\epsilon$ will be used entirely in heating up the water, i.e.,

$$\Delta\epsilon(z) = C'_v \rho(z) \Delta l \cdot \Delta T$$

where $C'_v = 4.184 C_v$ (Joules/(gr \times °C)), for C_v the specific heat in (calories/(gr \times °C)), which for water takes the value $C_v = 1$. In view of the previous equation and (3) we obtain:

$$\frac{dT}{dz} = \frac{p}{\nu} \frac{kd}{\eta C'_v} \frac{\epsilon''(T(z))}{\rho(0)} |E(z)|^2 \quad (4)$$

where use has been made of the fact that $\Delta T/\Delta t \rightarrow \nu dT/dz$, and that $\rho(z)$ is a constant in this region. In order to make optimum use of (4) it is convenient to express ϵ'' in terms of T explicitly. For instance, based on the numerical values of ϵ for water presented in Appendix B of [6], it is possible to fit the data to a suitable model for a given frequency. We find that a good model for ϵ'' is given by

$$\epsilon''|_{300 \text{ MHz}} \approx \frac{38.02}{5.42 + T} \quad (5a)$$

$$\epsilon''|_{3 \text{ GHz}} \approx \frac{\alpha}{\beta^T} \quad (5b)$$

$$\epsilon''|_{10 \text{ GHz}} \approx \frac{1100 - 8T}{30}, \quad (5c)$$

for $\beta = 2^{1/30}$, $\alpha = 12\beta^{25}$.

To illustrate how (5) can change the form of (4), we consider the case of 3 GHz for which after some manipulations, it can be shown that (5b) reduces (4) to

$$T(z) = \begin{cases} T_i + \frac{1}{L\ln\beta} \ln \left\{ 1 + \frac{1}{h} \int_0^z dz' \left| \frac{E(z')}{E_2} \right|^2 \right\}; & T \leq T_c \\ T_c; & z \geq h_c \end{cases} \quad (6a)$$

for

$$E_2 = \sqrt{\frac{\nu\eta C'_v \rho(0) \cdot (1^\circ C)}{pkdh L\ln\beta \epsilon''(T_c)}}. \quad (6b)$$

$$2) z > h_c, T = T_c$$

Now T cannot increase, and essentially all the energy $\Delta\epsilon$ goes into vaporization. Because the reduction of kinetic energy is minimum as compared with $\Delta\epsilon$, we obtain

$$\Delta\epsilon(z) = -\Delta l \cdot \Delta\rho \cdot L'_v$$

for $L'_v = 4184 L_v$ (Joules/gr), L_v denoting the heat of vaporization (cal/gr), which for water is $L_v \approx 540$. From (3) and the previous identity we obtain

$$\frac{d\rho}{dz} = -\frac{pkd}{\nu\eta L'_v} \frac{\rho(z)}{\rho(0)} \epsilon''(z) |E(z)|^2.$$

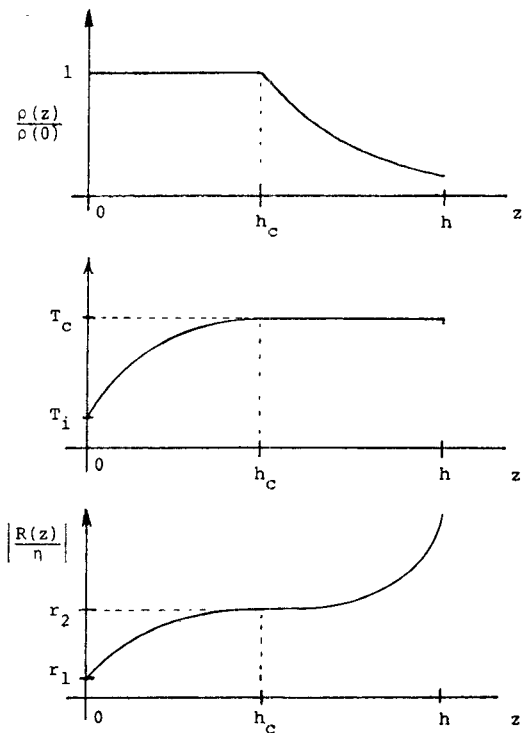


Fig. 4. Sketch of predicted profiles for density, temperature, and magnitude of sheet impedance.

In this region however, T is a constant and therefore ϵ'' is a constant. Use of this reduces the previous equation to

$$\frac{\rho(z)}{\rho(0)} = \begin{cases} 1; & z \leq h_c \\ e^{-\frac{1}{h} \int_{h_c}^z dz' \left| \frac{E(z')}{E_1} \right|^2}; & z \geq h_c \end{cases} \quad (7a)$$

for

$$E_1 = \sqrt{\frac{\nu\eta L'_v \rho(0)}{pkdh \epsilon''(T_c)}}. \quad (7b)$$

Note that T_c is used safely in this equation since E_1 plays a significant role only if $h_c < h$.

In view of the above, adequate operation of this device will be characterized by the profiles shown qualitatively in Fig. 4. $R(z)$ increases exponentially for $z > h_c$ because $\rho(z)$ decreases exponentially due to evaporation.

We now turn our attention to power calculations. First we calculate P , the power dissipated in a 1-m-wide sheet. This corresponds to integrating $\text{Re}\{E^* \cdot J\}$ over $z \in (0, h)$:

$$P(\text{watts}) = \frac{1}{\eta} \int_0^h dz |E(z)|^2 \text{Re} \left\{ \frac{1}{R(z)/\eta} \right\}. \quad (8)$$

In a time interval ν^{-1} the paper will advance 1 m, and since we are dealing with a 1-m-wide sheet, we conclude that the electromagnetic energy ϵ , utilized in "drying" a square meter of paper, is given by

$$\epsilon = P/\nu(\text{Joules}/m^2). \quad (9)$$

We now calculate P_e , the small amount of power escaping the dryer via transport of the stored electric energy in the sheet. First we determine ϵ_s , the electromagnetic energy stored per

TABLE I

T (°C)	R/η
25	3.228 -81.1°
55	3.698 -84.92°
85	4.429 -86.86°
100	4.8 -87.67°

unit volume in the sheet, when it is coming out of the dryer. This is given by $\text{Re}\{E \cdot D^* - B \cdot H^*\}$ evaluated at $z = h$. However, we can neglect the stored magnetic energy since we are dealing with a nonmagnetic material. Thus

$$\epsilon_s \approx \epsilon_o \epsilon'(T_o) |E(z = h)|^2 (\text{Joules}/m^3) \quad (10)$$

where $\epsilon_o \approx 8.85 \times 10^{-12}$ (farad/m). The volume of paper coming out of this 1-m-wide sheet in a second is equal to: $V = 1m \cdot \nu \cdot \{d\rho(h)/\rho(0)\}$, where the quantity in curly brackets accounts for the evaporation. Thus, since the electromagnetic energy coming out of the dryer in a second ($\epsilon_s V$), is equal to the (electric) power loss P_e , we have

$$P_e = \nu d \frac{\rho(h)}{\rho(0)} \epsilon_o \epsilon'(T_o) |E(z = h)|^2 (\text{watts}). \quad (11)$$

As will be seen later, numerical experiments have shown that P_e is indeed very small.

Finally, it should be mentioned that the electric field $E(z)$ is the true total field that satisfies Maxwell's equations in the presence of $R(z)$, which is unknown.

III. APPROXIMATIONS

Because of the complexity of the previous expressions, it is necessary to use some approximations in order to produce an estimate of the geometry and field requirements for satisfactory operation. This will result in an order of magnitude of the quantities involved and will serve as a starting point for parameter optimization, which will be made via numerical solution of Maxwell's equations and (4) and (7).

It has been shown in [7] that the Physical Optics approximation to the current induced in a resistive sheet is a good estimate for normal incidence, even for a parabolic resistive taper. Application of [7, (32)] to our case reveals that the total electric field in the sheet can be approximated by

$$E = J_2 \cdot R(z) = \frac{R(z)/\eta}{R(z)/\eta + 1/2} E_o. \quad (12)$$

Furthermore, in typical conditions it is estimated that $|R(z)| \gg \eta/2$. For example, for a typical $d = 1.27 \times 10^{-4}$ m, $p = 1/2$, $f = 3\text{GHz}$, and R/η prior to evaporation is given by Table I.

In presence of evaporation the values of R/η will be even higher. In deriving this table, use has been made of the fact that the values of ϵ' from [6] at $T = 25^\circ$, 55° , and 85°C , can be matched by the formula $\epsilon' = 85.5 - T/3$, at $f = 3\text{GHz}$. Also, the values of R at 100°C have been obtained by using the formulas for ϵ' and ϵ'' . In view of the above, we conclude that we can set $E(z) \approx E_o$ in the equations. We obtain:

$$\frac{\rho(z)}{\rho(0)} \approx e^{-(\frac{z-h_c}{h})(\frac{E_o}{E_1})^2 U(z-h_c)} \quad (13a)$$

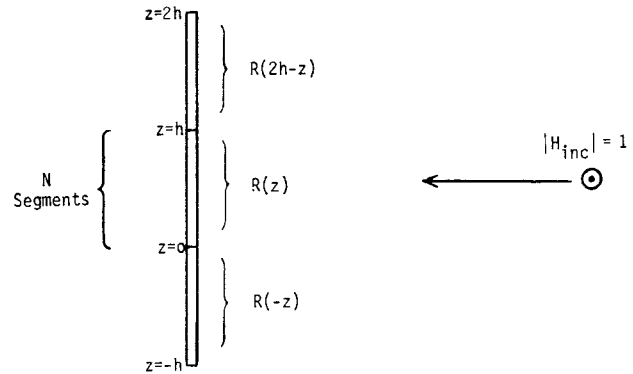


Fig. 5. Configuration for HPOLA.

$$T \approx \begin{cases} T_i + \frac{1}{\ln \beta} \ln \left\{ 1 + \frac{z}{h} \left(\frac{E_o}{E_2} \right)^2 \right\}; & T \leq T_c \\ T_c; & z \geq h_c, \end{cases} \quad (13b)$$

where U is the step function ($U(z) = 1$ if $z > 0$, and zero otherwise). Clearly, there exists a critical value of field amplitude $E_o = E_c$, which must be exceeded in order to have some evaporation. From (13b) we obtain (after setting $h_c = h$, because the maximum T occurs at $z = h$):

$$\frac{E_c}{E_2} = \sqrt{\beta^{T_c - T_i} - 1}, \quad (14)$$

which for normal conditions $T_c = 100^\circ\text{C}$, $T_i = 25^\circ\text{C}$ implies $E_c/E_2 \approx 2.158$. On the other hand, enforcement of (13b) at $z = h_c$ yields

$$\sqrt{\frac{h_c}{h}} \cdot E_o = E_c. \quad (15)$$

Similarly, evaluating (13a) at $z = h$ yields

$$\left(1 - \frac{h_c}{h} \right) \left(\frac{E_o}{E_1} \right)^2 = \ln \left[\frac{\rho(0)}{\rho(h)} \right]. \quad (16)$$

Furthermore, it can be shown from (6b) and (7b) that

$$\left(\frac{E_1}{E_2} \right)^2 = \frac{\ln \beta}{1^\circ\text{C}} \cdot \frac{L'_v}{C'_v} \beta^{T_c - T_i} = 12.4746 \beta^{T_c - T_i}, \quad (17)$$

and from (14)–(16), after eliminating E_o we get:

$$12.4746 \frac{h_c/h}{1 - h_c/h} \cdot \ln \left[\frac{\rho(0)}{\rho(h)} \right] = \frac{\beta^{T_c - T_i} - 1}{\beta^{T_c - T_i}} \quad (18)$$

which indicates that the thickness of the heating layer (h_c/h) needs to be small if significant drying is to be achieved. For instance, for typical $T_c = 100^\circ\text{C}$, $T_i = 25^\circ\text{C}$, (18) becomes

$$h/h_c = 1 + 15.15 \ln[\rho(0)/\rho(h)], \quad (19)$$

which is interesting since it implies that for a "dry" paper containing 1% of the original moisture ($\rho(0)/\rho(h) = 100$), $h \approx 71 h_c$, whereas for a paper being half as wet as originally ($\rho(0)/\rho(h) = 2$) we have $h \approx 11.5 h_c$. Thus we see that if significant drying is to be achieved, h_c/h is a very small number, which according to (15) implies that $E_o \gg E_c$, which is not convenient from the practical standpoint because E_c is large.

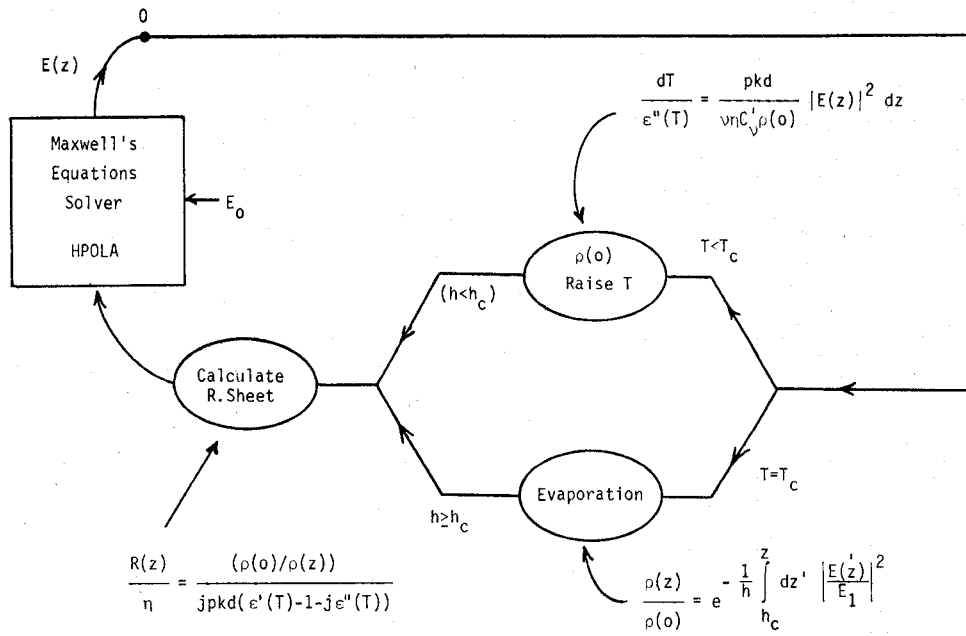
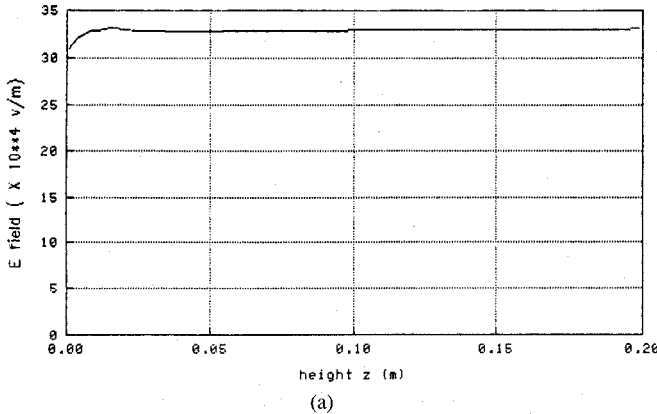
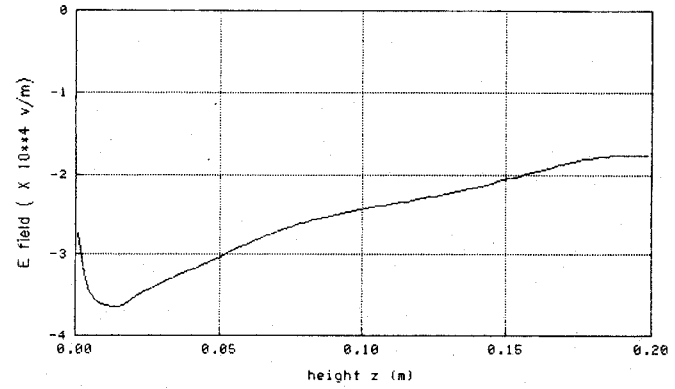


Fig. 6. Diagram of computational scheme.



(a)



(b)

Fig. 7. Electric field at the sheet via HPOLA and the analytical estimates presented in Fig. 7. (a) Real part of $E(z)$ profile. (b) Profile of $\text{Im}\{E(z)\}$.

IV. NUMERICAL IMPLEMENTATION

To solve this highly nonlinear problem, an iteration scheme is employed. The reason for this is the fact that a good original estimate of $E(z)$ is available from Physical Optics.

The geometry is that of a position dependent R-sheet bounded by two parallel plates, as depicted in Fig. 3. A sufficiently accurate (though not exact) solution to the field equations was obtained via the R-sheet portion of a company code, HPOLA, where a number of images of the original R-sheet were employed for normal incidence conditions, as shown in Fig. 5. In all cases considered, it was found that only two images were necessary, the solution converging immediately, which is consistent with the Physical Optics argument of [7]. N segments were used to model each inhomogeneous R-sheet.

Since HPOLA solves the problem for an incident magnetic field of unit amplitude, the $E(z)$ required in our computation

is obtainable from J , the electric currents of HPOLA, via:

$$E(z) = E_o J(z) \frac{R(z)}{\eta}; \quad z \in (0, h). \quad (20)$$

Only the current in the central sheet was considered.

To clarify the scheme, a brief block diagram description is presented in Fig. 6. We start the iteration at point 0, assuming $E(z) = E_o$; use this to calculate profiles $(T(z), \rho(z))$, which in turn are used to get $R(z)$, which when fed to HPOLA yields a new $E(z)$ and then go back to point 0. We then start a new cycle. The iteration stops when no sensible change in the profiles is observed. In practice, we have found that one iteration is sufficient in most cases due to the large values of associated R-sheet.

We now proceed to elaborate on a numerical experiment. Care must be exercised in selecting the correct operating voltage E_o , since too large a voltage will cause a very small h_c/h , which will prevent HPOLA from properly modeling the heat-

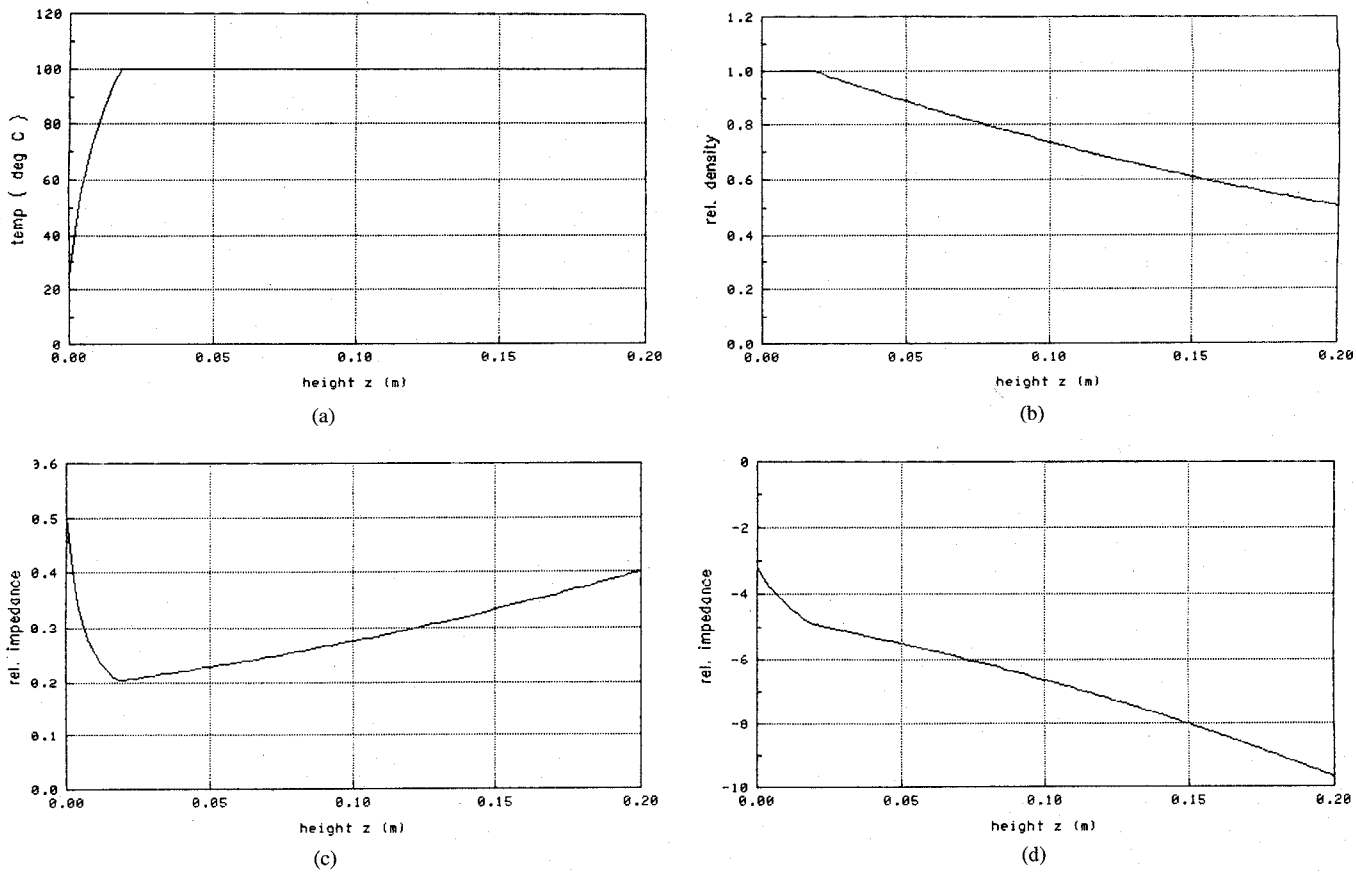


Fig. 8. Results after first iteration through HPOLA. (a) Temperature profile. (b) Density profile. (c) Real part of normalized impedance profile. (d) Imaginary part of normalized impedance profile. Further iterations resulted in negligible changes in the profiles shown here.

ing region $z \in (0, h_c)$ because the R-sheet will change rapidly in that region. On the other hand, too low a voltage will cause T_o to be less than T_c resulting in unsatisfactory operation.

For the following conditions: $T_i = 25^\circ\text{C}$, $T_o = 100^\circ\text{C}$, $\nu = 4.57 \text{ m/sec}$ ($\approx 900 \text{ feet/min}$), $d = 1.27 \times 10^{-4} \text{ m}$, $h = .2 \text{ m}$, $f = 3 \text{ GHz}$ ($\lambda = .1 \text{ m}$) and initial 50% moisture ($p = .5$), we find from the approximate formulae that the initial E-field is $E_c \approx 98 \text{ KV/m}$. For a 50% drying operation we have $\rho(0)/\rho(h) = 2$ and (19) yields $h/h_c \approx 11.5$, which when used in (16) yields $E_o \approx 333 \text{ KV/m}$.

The code we have developed is called PAPER, and it uses the output from HPOLA for each iteration. We initially run PAPER with the previous values of T_i , ν , d , h , f , p , $E_o = 333 \text{ KV/m}$ and $T_c = 100^\circ\text{C}$. The initial output from PAPER is the analytical estimate for $T(z)$ and $\rho(z)/\rho(0)$. Those two profiles resulted in the complex profile $R(z)/\eta$, whose magnitude $|R(z)/\eta|$ was found to be much larger than $1/2$, an assumption employed in simplifying (12).

HPOLA was run for the first iteration with $N = 60$ and $N = 100$, which roughly result in 5 and 8 unknowns for the $z \in (0, h_c)$ region of high activity. Using the previous values of $R(z)$, we run HPOLA, obtaining $J(z)$, which when inserted in (20) yield the electric field profile $E(z)$, whose real and imaginary parts are shown in Fig. 7(a) and (b), respectively. As expected, the real part of $E(z)$ is much larger than the imaginary part and outside the high activity region the field is very well represented by E_o . Very little difference was

observed between the $N = 60$ and $N = 100$ fields. Fig. 7 corresponds to $N = 100$.

These new values of $E(z)$ were fed to PAPER, which calculated the new profiles $T(z)$ and $\rho(z)$ shown in Fig. 8(a) and (b), respectively. Very little difference was observed between these new profiles and the analytical estimates, which explains why the new resistive profile shown in Fig. 8(c) and (d) is almost identical to the corresponding estimate. Further numerical work indicated that additional iterations were not necessary since the resistive profile remained essentially unchanged.

To give the reader an idea of how good the initial estimate was, we mention that for $N = 60$ we obtain a final moisture $\rho(h)/\rho(0) = .504431$, whereas $N = 100$ yield $\rho(h)/\rho(0) = .508500$. These numbers are quite close to the value of $.5$ imposed on the analytical estimate.

Finally we present some power figures. For $N = 100$, the dissipated power in a 1-m-wide sheet P , is given by $P = 405.29 \text{ KW}$. The energy E used in drying a square meter of paper is $E = 88.6848 \times 10^3 \text{ Joules}$. The power P_e escaping the dryer due to stored electric energy transport in the sheet is: $P_e \approx 14.85 \text{ mW}$. The numbers that have been presented are realistic as will be seen in the next section.

V. DISCUSSION

The numerical results are very encouraging due to the highly convergent nature of the scheme. The convergence is

remarkable in view of the fact that HPOLA gave only an approximate solution because only a few images were used.

Energy balance is another way of checking the accuracy of the previous results. In order to change the moisture of one square meter of paper from $\rho(o)$ to $\rho(h)$, requires first of all, an amount of energy equal to ΔE_T , in order to raise its temperature from T_i to T_c :

$$\Delta E_T = \rho(o) \cdot (T_c - T_i) \cdot C_v \quad (21)$$

plus an energy ΔE_E to cause evaporation from moisture $\rho(o)$ to $\rho(h)$:

$$\Delta E_E = [\rho(o) - \rho(h)] \cdot L_v. \quad (22)$$

Summing the two contributions we obtain that in the stationary case, a total energy of 90.43 KJ are needed ($\Delta E_T = 19.92$ KJ, $\Delta E_E = 70.51$ KJ). This energy should be compared with the total electromagnetic energy used in drying a square meter, which was presented in the previous section: $E = 88.68$ KJ. Note that the agreement is very good, within 2%. (The previous 90.43 KJ were obtained with $N = 100$; with $N = 60$ we obtained 91 KJ, thus for larger N we expect better agreement.)

The kinetic energy can be neglected in the analysis. To give an idea of the quantities involved, we compute the total kinetic energy lost per square meter:

$$\Delta E_K = \frac{1}{2} [\rho(o) - \rho(h)] \nu^2 \times 10^{-3} \text{ Joules} \quad (23)$$

which is equal in this case to $\approx .33$ Joules and is insignificant when compared with the total 90 KJ used in the evaporation.

In the numerical calculations we employed $L_v = 400$, rather than the better value [8, p. 306]: $L_v = 539.2$. Also the dependence of water density on temperature was ignored (dilation), even though the effect may be significant; for instance, [8, p. 273], at 4°C , the density is equal to $1\text{gr}/\text{cm}^3$, whereas at 100°C it is equal to $.958\text{ gr}/\text{cm}^3$.

Finally we mention that it may be worthwhile to seek lower frequencies of operation, where high fields are easier to generate. It is well known that past 1 GHz water shows strong absorption (see for example the graph of index of refraction and absorption coefficient for water as a function of the frequency, which is presented in [9]). However, there is some evidence [6, Appendix B] that at much lower frequencies (around 100 KHz), the water losses increase considerably and very possibly balance out the decrease in electrical thickness of the effective R-sheet, resulting in comparable values of R-sheet than at 3 GHz. Such behavior can be observed from the materials table of [6, Appendix B] where one can also notice that at 100 KHz, the losses increase with the temperature (not

so at 3 GHz), which is a very desirable property since h_c is usually much less than h , i.e., most energy is delivered to the sheet when it is hot, during evaporation.

ACKNOWLEDGMENT

The author wishes to express his appreciation to Dr. Nick Damaskos, President of Damaskos, Inc., for his kind interest in this work. Thanks are extended to Malcolm Lundin for the programming support, and to the anonymous reviewers for their constructive criticism and valuable references.

REFERENCES

- [1] J. R. Wait, "Focused heating in cylindrical targets: Part I," *IEEE Trans. Microwave Theory Tech.*, vol. MTT-33, no. 7, pp. 647-649, July 1985.
- [2] J. R. Wait, and M. Lumori, "Focused heating in cylindrical targets: Part II," *IEEE Trans. Microwave Theory Tech.*, vol. MTT-34, no. 3, pp. 357-359, Mar. 1986.
- [3] F. Bardati, "Time-dependent microwave heating and surface cooling of simulated living tissues," *IEEE Trans. Microwave Theory Tech.*, vol. MTT-29, no. 8, pp. 825-828, Aug. 1981.
- [4] S. C. Kashyap, and J. G. Dunn, "A waveguide applicator for sheet materials," *IEEE Trans. Microwave Theory Tech.*, pp. 125-126, Feb. 1976.
- [5] W. van Loock, "Microwave applications within the European communities," in *Proc. 20th Annual Microwave Symp. Int. Microwave Power Institute*, pp. 78-89, Chicago, IL, Aug. 26-28, 1985.
- [6] R. F. Harrington, *Time Harmonic Electromagnetic Fields*. New York: McGraw-Hill, 1961.
- [7] R. L. Haupt and V. V. Liepa, "Synthesis of tapered resistive strips," *IEEE Trans. Antennas Propagat.*, vol. AP-35, no. 11, pp. 1217-1225, Nov. 1987.
- [8] J. J. Tuma, *Handbook of Physical Calculations*. New York: McGraw-Hill, 1976.
- [9] J. D. Jackson, *Classical Electrodynamics*. New York: Wiley, 1975.
- [10] Part of an unpublished internal report, "An electromagnetic paper dryer," Damaskos, Inc., Mar. 31, 1989.
- [11] M. Hamid *et al.*, "Microwave package for the control of moisture content and insect infestation of grain," U.S. Patent No. 3,611,582, Oct. 12, 1971.
- [12] M. Hamid, "Microwave drying of clothes," *J. Microwave Power & Electromagnetic Energy*, vol. 26, no. 2, pp. 107-114, 1991.
- [13] W. Meyer and W. M. Schilz, "Feasibility study of density—Independent moisture measurement with microwave," *IEEE Trans. Microwave Theory Tech.*, vol. MTT-29, no. 7, pp. 732-739, July 1981.
- [14] W. Schilz and B. Schiek, "Microwave systems for industrial measurement," *Advances Electron.*, vol. 55, p. 309, 1981.
- [15] A. W. Kraszewski, "Microwave aquametry—Needs and perspectives," *IEEE Trans. Microwave Theory Tech.*, vol. 39, no. 5, pp. 828-835, May 1991.
- [16] R. J. King, K. V. King, and K. Woo, "Microwave moisture measurement of grains," *IEEE Trans. Instrumentation Meas.*, vol. 41, no. 1, pp. 111-115, Feb. 1992.
- [17] R. F. Harrington and J. R. Mautz, "An impedance sheet approximation for thin dielectric shells," *IEEE Trans. Antennas Propagat.*, vol. AP-23, no. 4, pp. 531-534, July 1975.

J. Cesar Monzon (S'79-M'79-S'80-M'81-M'85), photograph and biography not available at the time of publication.